

Safe CO₂ threshold limits for indoor long-range airborne transmission control of COVID-19

Article

Accepted Version

Creative Commons: Attribution-Noncommercial-No Derivative Works 4.0

Lyu, X., Luo, Z. ORCID: <https://orcid.org/0000-0002-2082-3958>, Shao, L. ORCID: <https://orcid.org/0000-0002-1544-7548>, Awbi, H. and Lo Piano, S. ORCID: <https://orcid.org/0000-0002-2625-483X> (2023) Safe CO₂ threshold limits for indoor long-range airborne transmission control of COVID-19. *Building and Environment*, 234. 109967. ISSN 03601323 doi: <https://doi.org/10.1016/j.buildenv.2022.109967> Available at <https://centaur.reading.ac.uk/110045/>

It is advisable to refer to the publisher's version if you intend to cite from the work. See [Guidance on citing](#).

To link to this article DOI: <http://dx.doi.org/10.1016/j.buildenv.2022.109967>

Publisher: Elsevier

All outputs in CentAUR are protected by Intellectual Property Rights law, including copyright law. Copyright and IPR is retained by the creators or other copyright holders. Terms and conditions for use of this material are defined in the [End User Agreement](#).

www.reading.ac.uk/centaur

CentAUR

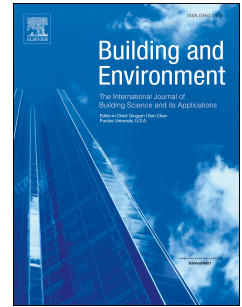
Central Archive at the University of Reading

Reading's research outputs online

Journal Pre-proof

Safe CO₂ threshold limits for indoor long-range airborne transmission control of COVID-19

Xiaowei Lyu, Zhiwen Luo, Li Shao, Hazim Awbi, Samuele Lo Piano



PII: S0360-1323(22)01197-0

DOI: <https://doi.org/10.1016/j.buildenv.2022.109967>

Reference: BAE 109967

To appear in: *Building and Environment*

Received Date: 15 October 2022

Revised Date: 16 December 2022

Accepted Date: 29 December 2022

Please cite this article as: Lyu X, Luo Z, Shao L, Awbi H, Lo Piano S, Safe CO₂ threshold limits for indoor long-range airborne transmission control of COVID-19, *Building and Environment* (2023), doi: <https://doi.org/10.1016/j.buildenv.2022.109967>.

This is a PDF file of an article that has undergone enhancements after acceptance, such as the addition of a cover page and metadata, and formatting for readability, but it is not yet the definitive version of record. This version will undergo additional copyediting, typesetting and review before it is published in its final form, but we are providing this version to give early visibility of the article. Please note that, during the production process, errors may be discovered which could affect the content, and all legal disclaimers that apply to the journal pertain.

© 2022 Published by Elsevier Ltd.

1 Manuscript revised to Building and Environment, Dec 2022

2

3 **Safe CO₂ Threshold Limits for Indoor Long-range Airborne Transmission**

4 **Control of COVID-19**

5 Xiaowei Lyu¹, Zhiwen Luo^{2*}, Li Shao¹, Hazim Awbi¹, Samuele Lo Piano¹

6 1. School of the Built Environment, University of Reading, UK

7 2. Welsh School of Architecture, Cardiff University, UK

8 Correspondence: Prof Zhiwen Luo (LuoZ18@Cardiff.ac.uk)

9 **Abstract:** CO₂-based infection risk monitoring is highly recommended under the current
10 COVID-19 pandemic. However, the CO₂ monitoring thresholds proposed in the literature are
11 mainly for spaces with fixed occupants. Determining CO₂ threshold is challenging in spaces
12 with changing occupancy due to the co-existence of quanta and CO₂ remaining from the
13 previous occupants. Here, we propose a new calculation framework to derive safe excess CO₂
14 thresholds (above outdoor level), C_t , for various spaces with fixed/changing occupancy and
15 analyze the uncertainty entailed. Common indoor spaces were categorized into three scenarios
16 according to their occupancy condition, e.g., fixed or varying infection ratios
17 (infectors/occupants). We proved that rebreathed fraction-based model can be directly applied
18 for C_t derivation in the cases of a fixed infection ratio (Scenario 1 and Scenario 2). In the case
19 of varying infector ratios (Scenario 3), C_t derivation has to follow the general calculation
20 framework due to the existence of initial quanta/excess CO₂. Otherwise, significant bias can be

21 caused for C_t (e.g., 260 ppm) when infection ratio varies remarkably. C_t significantly varies
 22 with specific space factors such as occupant number, activities, and community prevalence,
 23 e.g., 7 ppm for gym and 890 ppm for lecture hall, indicating C_t should be determined on a case-
 24 by-case basis. An uncertainty of C_t up to 6 orders of magnitude was found for all cases due to
 25 uncertainty in emissions of quanta and CO_2 , thus emphasizing the role of accurate emissions
 26 data in obtaining C_t .

27

28 **Keywords:** infection risk control, CO_2 monitoring, initial quanta, uncertainty analysis

29

Nomenclature	
B	Breathing rate, m ³ /h
$C_{CO_2,i}$	CO_2 concentration for occupancy stage i , ppm
$C_{Cin,i}$	Initial CO_2 concentration for occupancy stage i , ppm
$C_{q,i}$	Quanta concentration for occupancy stage i , quanta/m ³
$C_{qin,i}$	Initial quanta concentration for occupancy stage i , quanta/m ³
C_t	Safe excess CO_2 threshold, ppm
C_{t50}	Median safe excess CO_2 threshold, ppm
E_{co_2}	CO_2 emission rate, mL/s
E_q	Quanta emission rate, quanta/h
I_i	Infector number for occupancy stage i
N_{ave}	Average occupant number
N_i	Occupant number for occupancy stage i
P_i	Infection risk for occupancy stage i
P_t	Predefined infection risk threshold
P_l	Community prevalence
T_i	Exposure time for occupancy stage i , h
V	Space volume, m ³
λ_i	Air change rate for occupancy stage i , h ⁻¹

30

31 1. Introduction

32 COVID-19, as a novel coronavirus disease, has caused a worldwide pandemic spreading
33 since the end of 2019 (Chen et al., 2020). Indoor transmission control is the key to prevent the
34 spread of the SARs-CoV-2 virus due to a higher transmission risk indoors than outdoors (Qian
35 et al., 2020). The four main transmission routes in indoor environments are droplet-borne,
36 fomite, short-range airborne, and long-range airborne (Li, 2021; Wei and Li, 2016). Although
37 short-range airborne transmission route was inferred to be the dominant route in close contact
38 (Chen et al., 2020), long-range airborne transmission was revealed to more likely induce
39 outbreaks in poorly ventilated and confined indoor spaces (Peng et al., 2022). Thus, it is of
40 primary importance to monitor and control long-range airborne transmission for indoor
41 environment.

42 The exhaled infectious aerosols contributing to long-range airborne transmission are difficult
43 to detect, and can travel a long distance in indoor environment. Therefore, a detectable indicator
44 for transmission risk is urgently needed to effectively monitor long-range airborne transmission.
45 CO_2 that can be easily monitored through low-cost sensors (Peng and Jimenez, 2021) has been
46 recommended as risk indicator for long-range airborne transmission because it can both reflect
47 the indoor ventilation condition and the quanta concentration (Persily et al, 2022). Accordingly,
48 safe CO_2 thresholds are defined as the maximum CO_2 concentration level under which the
49 indoor space is at an acceptable infection risk. Such information is useful to guide the design
50 of infection-resilient buildings.

51 Treating CO_2 as an indicator for indoor ventilation performance, recent studies made use of
52 CO_2 thresholds for risk control based on prevailing ventilation standards with a target of
53 acceptable indoor air quality (IAQ) but not infection risk (CIBSE, 2021; SAGE-EMG, 2021;

54 REHVA, 2021). ASHRAE does not recommend a specific value of threshold (Persily et al.,
55 2022), although other organizations have suggested specific thresholds of 800 ppm (SAGE-
56 EMG, 2020; CDC, 2021) or 800-1000 ppm (REHVA, 2021) to ensure a safe indoor
57 environment. However, whether a fixed CO_2 threshold could guarantee a low infection risk
58 for all spaces is questionable considering factors such as occupancy level and respiratory
59 activity can all affect the value of it (Peng and Jimenez, 2021).

60 Moving beyond the assessment of CO_2 as a mere indicator of indoor ventilation condition,
61 CO_2 can also be used to directly reflect quanta concentration as CO_2 and virus-laden aerosols
62 can be co-produced and co-inhaled by human. Therefore, CO_2 thresholds can be calculated
63 backward by pre-defining an acceptable infection risk level (Hou et al., 2021; Peng and
64 Jimenez, 2021). Indoor airborne transmission risk can be maintained under the predefined risk
65 level in as much indoor CO_2 concentration can be maintained below the derived threshold.
66 Occupancy level and respiratory activity for a particular indoor space can all be factored in this
67 backward calculation process (Hou et al., 2021; Peng and Jimenez, 2021; Rudnick and Milton,
68 2003). In the literature, the derived thresholds were found to be highly sensitive to factors such
69 as activity level and community prevalence, making CO_2 thresholds varying across different
70 indoor spaces (Peng and Jimenez, 2021). For example, the reference excess CO_2 threshold
71 (above outdoor level) for classroom amounts to only about 150 ppm, while this figure is ten-
72 fold for supermarket (Peng and Jimenez, 2021). This indicates that the CO_2 thresholds should
73 be determined case by case, instead of setting a fixed value for all spaces.

74 In addition, most proposed thresholds are for spaces with fixed occupancy level under the
75 assumption of no initial quanta/excess CO_2 (Hou et al., 2021; Peng and Jimenez, 2021; Rudnick

76 and Milton, 2003). For spaces with variable occupancy, some of quanta/ CO_2 released by the
77 previous group of occupants can remain in the space and become initial quanta/ CO_2 when the
78 next group occupies the space, hence increasing the infection risk for the current occupants.
79 The initial quanta is essential for defining CO_2 threshold, but it is difficult to estimate as it
80 requires information of ventilation condition and occupancy profile of previous occupancy
81 stage. Hence, how to account for initial quanta/excess CO_2 in spaces with changing occupancy
82 in infection risk assessment remains an unsolved question (Mittal et al., 2020b; Wei and Li,
83 2016).

84 Finally, emissions of quanta and CO_2 are two important parameters in determining the CO_2
85 threshold, but they have inter-individual variation and can also be affected by factors such as
86 age and gender (Buonanno et al., 2020a; Persily and de Jonge, 2017; Good et al., 2021). For
87 instance, the viral load of super-spreader can be 10 times higher than the mean level of normal
88 infectious subjects (Lelieveld et al., 2020), which may indicate a higher quanta emission (Ke
89 et al., 2021, 2022). Different values of quanta and CO_2 emission were adopted by previous
90 studies for CO_2 threshold derivation, e.g., from 0.37 quanta/h to 100 quanta/h for classrooms
91 (Buonanno et al., 2020a; Bazant et al., 2021; Hou et al., 2021; Peng and Jimenez, 2021). The
92 effect on the uncertainty on the emissions of quanta and CO_2 on defining a CO_2 threshold
93 should be further analyzed. The present study aims to provide a new calculation framework to
94 derive safe excess CO_2 thresholds (C_i) by considering initial quanta/excess CO_2 and
95 changing/fixed occupancy patterns for different indoor spaces, as well as propagating the
96 uncertainty of these input variables.

97 **2. Methodology**

98 *2.1 General calculation framework*

99 Our model is based on four assumptions for indoor mass balance equations for CO_2 and
 100 quanta (Hou et al., 2021): 1) both CO_2 and quanta are well mixed and evenly distributed in
 101 the air; 2) indoor excess CO_2 is released by human exhalation only, with no other indoor
 102 sources; 3) CO_2 emission rate and quanta emission rate are both constant (i.e., not time
 103 dependent); 4) the loss of quanta is mainly due to ventilation, other elimination mechanisms
 104 such as deposition, filtration and inactivation are neglected.

105 In deriving C_t for spaces with changing occupants, we consider a sequence of occupancy
 106 stages, $S_i(I_i, N_i, T_i)$. Stage i represents an indoor space (with the volume of V) being occupied
 107 by a number of occupants (N_i) with infectors (I_i) for a duration of time (T_i). $i=1$ represents the
 108 start of the occupancy: N_1 occupants (with I_1 infectors) stay in this indoor space for a period of
 109 T_1 , with no people inside prior to N_1 occupants. The introduction of various occupancy stages
 110 aims to consider the virus released and still in the air from previous occupancy stages (the
 111 initial quanta). This is fundamentally different from previous studies which only considered
 112 one-off occupancy or fixed occupancy throughout the exposure period of interest.

113 The general calculation process of C_t for one occupancy stage of a space is given as follows.

114 Long-range transmission risk for occupancy stage i is modeled through a Wells-Riley model
 115 (Riley et al., 1978) amended by Gammitoni and Nucci (1997) to assess infection risk through
 116 unsteady-state quanta concentration:

$$117 \quad P_i = 1 - e^{-B \int_0^{T_i} C_{q,i}(t) dt} \quad (1)$$

118 Quanta concentration in Equation (1) is modeled through transient mass balance equation:

$$119 \quad \frac{dC_{q,i}}{dt} = \frac{I_i E_q}{V} - \lambda_i C_{q,i} \quad (2)$$

120 Equation (2) can be analytically solved as:

$$121 \quad C_{q,i}(t) = \left(C_{qin,i} - \frac{I_i E_q}{\lambda_i V} \right) e^{-\lambda_i t} + \frac{I_i E_q}{\lambda_i V} \quad (3)$$

122 To control transmission risk of stage i under an acceptable low level, a risk threshold of P_t
 123 needs to be initially determined. Based on P_t , a required ACH (air change rate, λ_i) can be
 124 derived by substituting Equation (3) into Equation (1), λ_i should be no less than the derived
 125 value to keep transmission risk under P_t .

126 Indoor excess CO_2 concentration is also dominated by ACH, hence it reflects the ventilation
 127 condition of stage i .

128 Indoor excess CO_2 concentration for stage i is determined by mass balance equation (4):

$$129 \quad \frac{dC_{CO_2,i}}{dt} = \frac{N_i E_{CO_2}}{V} - \lambda_i C_{CO_2,i} \quad (4)$$

130 Equation (4) is solved as:

$$131 \quad C_{CO_2,i}(t) = \left(C_{Cin,i} - \frac{N_i E_{CO_2}}{\lambda_i V} \right) e^{-\lambda_i t} + \frac{N_i E_{CO_2}}{\lambda_i V} \quad (5)$$

132 Substituting the required ACH that is backward calculated from transmission risk threshold
 133 into Equation (5), the time-averaged indoor excess CO_2 concentration ($C_{CO_2,i}$) during T_i is
 134 exactly C_t for stage i (Hou et al., 2021; Bazant et al., 2021):

$$135 \quad C_t = \frac{1}{T_i} \int_0^{T_i} C_{CO_2,i}(t) dt \quad (6)$$

136 When indoor excess CO_2 concentration is below the reference threshold C_t , sufficient
 137 ventilation can be promised to keep long-range transmission risk for occupancy stage i under
 138 the risk level of P_t .

139 Further, for different occupancy stages, C_t can be derived by following the steps mentioned
 140 above considering the existence of initial quanta/excess CO_2 , see Equation (3) and Equation
 141 (5). Starting from occupancy stage 1 without initial quanta/excess CO_2 , a required ACH (λ_i)

142 can be easily obtained following the general calculation process. For occupancy stage 2, the
143 initial quanta and initial excess CO_2 can be estimated based on the ACH derived in occupancy
144 stage 1 (λ_1) under the assumption that excess CO_2 during occupancy stage 1 has been controlled
145 under the reference threshold, C_t for occupancy stage 2 can then be obtained according to the
146 calculation framework. Repeating these steps, i.e. by taking the derived ACH of previous
147 occupancy stage to estimate initial quanta/excess CO_2 for present stage, C_t can be calculated
148 iteratively for all the occupancy stages modeled.

149 *2.1.1 Infection Risk Threshold P_t*

150 The infection risk threshold P_t is of great importance as it dominates the safety levels of the
151 indoor environment. It can be defined in two ways, either by using a constant value for all
152 environment - such as 1%, 0.1% (Dai and Zhao, 2020) or even 0.01% (Peng and Jimenez -
153 2021) or to determine P_t based on reproductive number (R_A) where R_A is the average number
154 of secondary cases caused by one infector in a given susceptible population in indoor
155 environment. In the latter, the value of P_t is dominated by the number of occupants and can be
156 a large and inconvincible value when occupant number is small (Ma et al., 2018; Furuya et al.,
157 2009). In this study, we use a constant value of $P_t = 0.01\%$ as suggested in Peng and Jimenez
158 (2021), which is reasonable for most occupancy stages when the number of occupants is less
159 than 10,000.

160 *2.2 Designed Scenarios*

161 Three scenarios were identified to calculate C_t :

162 1) Regularly attended space with fixed occupancy level and the same group of people as
 163 occupants, so that $N_1=N_2=...$ (e.g., a lecture room used by a certain group of students)
 164 (Burridge et al., 2021; Vouriot et al., 2021) ;

165 2) Non-regularly attended space with constant infection ratio ($I_1/N_1=I_2/N_2=...=I_i/N_i$),
 166 different groups of people as occupants, and with high occupancy level (e.g., shopping center,
 167 train station);

168 3) Non-regularly attended space with changing infection ratio ($I_1/N_1 \neq I_2/N_2 \neq ... \neq I_i/N_i$) and low
 169 occupancy level (e.g., gym, train coach).

170 All these scenarios are widely experienced in real-life situations.

171 2.2.1 Scenario 1: Regularly attended spaces

172 We determined the number of infectors I_i for Scenario 1 according to both the indoor
 173 occupancy level (N_i) and local community prevalence (P_I). The expected I_i is defined as max
 174 $\{1, P_I N_i\}$. When with a low indoor occupancy level or a low community prevalence, the value
 175 of $P_I N_i$ can be less than 1, under such condition, I_i is assumed to be equal to 1, Otherwise, I_i is
 176 assumed to be $P_I N_i$ to reflect the real local infection condition.

177 Derived from mass balance equations, quanta concentration and excess CO_2 concentration
 178 were found to have a constant proportion during all the occupancy stages, only affected by
 179 infection ratio and emissions, see Equation (7) (Full derivation details can be found in
 180 Supplementary Information). As long as the infection ratio and emissions do not change during
 181 the occupancy stages, the proportion remains unchanged as well, hence:

$$\frac{C_{q,1}(t)}{C_{CO_2,1}(t)} = \frac{C_{q,2}(t)}{C_{CO_2,2}(t)} = \dots = \frac{I_i}{N_i} \frac{E_q}{E_{CO_2}} \quad (7)$$

Under these circumstances, infection risk for stage i Eq (1) can be revised as below

$$P_i = 1 - e^{-B \frac{I_i}{N_i} \frac{E_q}{E_{CO_2}} \int_0^{T_i} C_{CO_2,i}(t) dt} \quad (8)$$

Equation (8) can be treated as the classical rebreathed fraction (RF) -based infection risk model derived by Rudnick and Milton (2003), with $BC_{CO_2,i}(t)/E_{CO_2}$ representing the rebreathed fraction. This derivation proved that rebreathed fraction (RF) -based model can account for the impact of initial quanta/excess CO_2 in risk assessments for spaces with fixed occupants.

Based on Equation (8), the time averaged value C_t for occupancy stage i can then be derived as:

$$C_t = \frac{E_{CO_2} N_i}{E_q T_i B I_i} \ln \left(\frac{1}{1 - P_t} \right) \quad (9)$$

2.2.2 Scenario 2: Non-regularly attended spaces with constant infection ratios

In Scenario 2, we assumed that community prevalence (P_t) can be directly used to represent indoor infection ratio due to the high occupancy level ($I_1/N_1 = I_2/N_2 = \dots = P_t$). The proportion between $C_{q,i}$ and excess $C_{CO_2,i}$ also become constant due to the constant infection ratio among occupancy stages (Detailed derivation process can be found in Supplementary Information):

$$\frac{C_{q,1}(t)}{C_{CO_2,1}(t)} = \frac{C_{q,2}(t)}{C_{CO_2,2}(t)} = \dots = P_t \frac{E_q}{E_{CO_2}} \quad (10)$$

Similar as Scenario 1, the infection risk and excess CO_2 threshold can then be derived as:

$$P_i = 1 - e^{-BP_t \frac{E_q}{E_{CO_2}} \int_0^{T_i} C_{CO_2}(t) dt} \quad (11)$$

$$C_t = \frac{E_{CO_2}}{E_q T_i B P_t} \ln \left(\frac{1}{1 - P_t} \right) \quad (12)$$

Equation (11) can be treated as an extension of the classical RF-based infection risk model.

The generality of the original model is extended from scenarios with fixed occupants (scenario

204 1) to scenarios with varying occupancy levels (scenario 2), with initial quanta/excess CO_2 to
205 be taken into account. It should be noted that T_i in Scenario 2 is usually hard to monitor as the
206 occupancy level keeps changing. An alternative method is to predefine it according to the
207 characteristics of different spaces. For example, T_i could be set as 35 min for check-in hall and
208 100 min for departure hall according to the average dwelling times measured in an airport (Mihi
209 et al., 2018).

210 2.2.3 Scenario 3: Non-regularly attended spaces with changing infection ratios

211 In Scenario 3, indoor infection ratio cannot be represented by P_i due to the relatively low
212 occupancy level. I_i is therefore recommended as the maximum value of $\{1, N_i P_i\}$ to provide a
213 safe indoor environment (as Scenario 1). In these circumstances, the infection ratio would
214 change among the occupancy stages and quanta concentration, and it would not be represented
215 by excess CO_2 concentration: C_i derivation needs to follow the general calculation process (see
216 Part 2.1).

217 It should be noted that the general calculation process does not require the field measurement
218 of ACH but relies on a known occupancy profile including the number of occupants and the
219 duration of occupancy for all the occupancy stages. Thus, this method may be more suitable
220 for spaces in Scenario 3 where the occupancy profile of N_i and T_i of each occupancy stage can
221 be monitored simultaneously or obtained before the spaces being occupied such as the rail train
222 or theatre.

223 2.3 Uncertainty analysis and inputs

224 Uncertainty analysis was carried out considering E_q and E_{CO_2} have interindividual variation

225 and can vary with gender, age, leading uncertainty to C_t . The probability density functions
 226 (PDF) of E_q for three different activities are from recent research of Buonanno et al. (2020a),
 227 where they found the quanta emission follows a log10-normal distribution, see Table 1. E_{CO_2}
 228 was also assumed to be lognormally distributed with a standard deviation equal to 20% of its
 229 mean (Molina and Jones, 2021). The mean value for the distribution is calculated as the average
 230 value of E_{CO_2} of female and male individuals aged 30 to 40 years (the most frequent age cohort)
 231 with a specific metabolic equivalent (Persily and de Jonge, 2017). The metabolic equivalent
 232 for E_{CO_2} is specified by different activity levels, specifically, 1.5 met for sedentary activity, 3
 233 met for light activity, 9 met for heavy activity (Ainsworth et al., 2000). Latin Hypercube
 234 sampling (LHS) (Fang et al. 2005) was used to generate a total of 30,000 samples from
 235 emissions of quanta and CO_2 due to its advantage in reflecting the true underlying distribution
 236 of inputs with a smaller sample size. Monte Carlo simulations (Sobol', 1994) were used to
 237 propagate and quantify the uncertainty in predictions.

238 **Table 1. Inputs for Uncertainty Analysis. Distribution mean and standard deviation in brackets**

Activity	Quanta emission PDF (quanta/h)	CO ₂ emission PDF (mL/s)
Sedentary - breathing	LN10 (-0.429, 0.720)	LN (5.05, 1.01)
Light activity - speaking	LN10 (0.698, 0.720)	LN (10.10, 2.02)
Heavy activity - breathing	LN10 (0.399, 0.720)	LN (34.20, 6.84)

239 Typical indoor environments were selected for each scenario based on factors such as
 240 occupancy level, infection ratio etc. (Tables 2 and 3). Cases in Scenario 1 have a fixed but
 241 different number of occupants considering that this is a dominant parameter in deriving C_t in
 242 Scenario 1, see Equation (9). It should be noted that the case of lecture hall in Scenario 1 has 3
 243 infectors due to its high occupancy level, whereas other cases have only 1 infector due to the

244 relatively low occupancy level. In Scenario 2 a shopping center was taken as case study with
 245 variable levels of community prevalence, which were adopted from three different COVID-19
 246 periods in the UK for 2020 (Pouwels et al., 2021) to represent relatively small (0.06%), median
 247 (0.4%) and high (1%) community prevalence, among which the highest level of community
 248 prevalence was adopted for Scenario 1 and Scenario 3. Two cases with low and changing
 249 occupancy levels were selected for Scenario 3 (i.e., train coach and gym room). As regards
 250 occupancy stages, only one stage was included for cases in Scenario 1 and Scenario 2 whereas
 251 five occupancy stages were included for cases in Scenario 3 to take into account the variability
 252 in C_t due to the impact of initial quanta/excess CO_2 . Different categories of activities were
 253 considered in the cases of the different scenarios. Cases in Scenario 1 are assumed to have
 254 “sedentary activity - breathing” typical of people sitting or standing in office or classroom
 255 environments. Cases in Scenario 2 are assumed to have “light activity - speaking”, considering
 256 that people are usually walking in the shopping center and talking to each other. For scenario
 257 3, two activities are included to explore the effects of activity level on C_t derivation, specifically,
 258 “sedentary activity – breathing” for the train coach and “moderate activity – breathing” for
 259 gym. The breathing rates (B) corresponding to different physical activity level is adopted are
 260 from previous research (Adams, 1993).

261 **Table 2. Inputs of uncertainty analysis for Scenario 1 and Scenario 2.**

Case	Volume (m ³)	Infector number	Occupant number	Exposure time (h)	Community prevalence	Breathing rate (m ³ /h)
Scenario 1						
Classroom	231	1	30	1	1%	0.54
Lecture classroom	270	1	65	1	1%	0.54
Lecture hall	540	3	300	1	1%	0.54
Open-plan office	594	1	20	1	1%	0.54
Scenario 2						

Shopping center	2040	-	-	1	0.06%, 0.4%, 1%	1.38
-----------------	------	---	---	---	-----------------	------

262 **Table 3. Inputs of uncertainty analysis for Scenario 3**

Scenario 3	Stage 1	Stage 2	Stage 3	Stage 4	Stage 5
Train coach (300 m³)					
Infector number	1	1	1	1	1
Occupant number	20	40	80	40	20
Exposure time (h)	1	1	1	1	1
Community prevalence	1%	1%	1%	1%	1%
Breathing rate (m ³ /h)	0.54	0.54	0.54	0.54	0.54
Gym (600 m³)					
Infector number	1	1	1	1	1
Occupant number	5	10	20	10	5
Exposure time (h)	1	1	1	1	1
Community prevalence	1%	1%	1%	1%	1%
Breathing rate (m ³ /h)	3.30	3.30	3.30	3.30	3.30

263 **3. Results**264 *3.1 Safety excess CO₂ threshold varies in different scenarios*

265 For Scenario 1, the number of occupants (N_i) is the dominant factor governing C_t that scales
266 with it (see Equation (9)). C_t for cases with different N_i in Scenario 1 (regularly attended spaces)
267 have substantial differences, see Figure 1(a). The highest C_{t50} (the median value of C_t) occurs
268 in lecture hall (890 ppm), followed by lecture classroom (580 ppm), classroom (270 ppm), the
269 lowest one is in office environment (180 ppm), although significant overlaps exist in the output
270 distributions (Figure 1(a)).

271 For Scenario 2, instead of N_i , C_t is dominated by community prevalence (P_I), as C_t is
272 inversely proportional to P_I (see Equation (12)). Three different values of P_I (i.e., 0.06%, 0.4%
273 and 1%) are adopted to derive C_t and the results are showed in Figure 1(b). The highest C_{t50} of
274 870 ppm refers to the lowest P_I of 0.06% and the lowest C_{t50} of 50 ppm to the highest P_I of 1%.

275 For Scenario 3, the changing infection ratios lead to different values of C_t for different

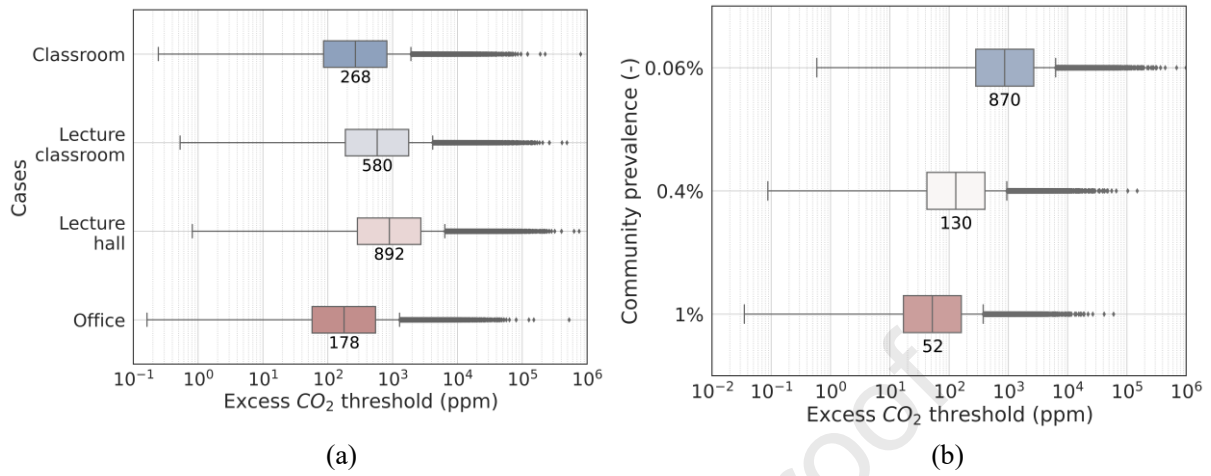
276 occupancy stages. For train coach, C_{t50} are approx. 180 ppm, 320 ppm, 650 ppm, 410 ppm and
277 200 ppm corresponding to infection ratios of 1/20, 1/40, 1/80, 1/40 and 1/20 for the five stages
278 in sequence, while they are 7 ppm, 15 ppm, 30 ppm, 15 ppm and 7 ppm for gym environment
279 corresponding to infection ratios of 1/5, 1/10, 1/20, 1/10 and 1/5. The changing infection ratios
280 can lead to different C_t values in different stages mainly because the existence of initial
281 quanta/excess CO_2 . For instance, for Stage 2 and Stage 4 of train coach with the same occupant
282 number of 40, C_{t50} should be same if initial quanta/excess CO_2 is not considered, but in fact the
283 difference of C_{t50} between the two occupancy stages reaches approx. 80 ppm due to the impact
284 of initial quanta/excess CO_2 .

285 In addition, the general cases in Scenario 3 also proves that activity level is another major
286 factor which can affect the derived thresholds, see Figure 1(c). C_t for gym with a high activity
287 level is much lower than that for train coach with a sedentary activity level due to relative high
288 activity level in gym environment (hence, high emission rate for quanta). This agrees with
289 previous studies (Chen et al., 2022; Jia et al., 2022) that there should be much higher restriction
290 in spaces with high activities such as gym to control airborne infection risk.

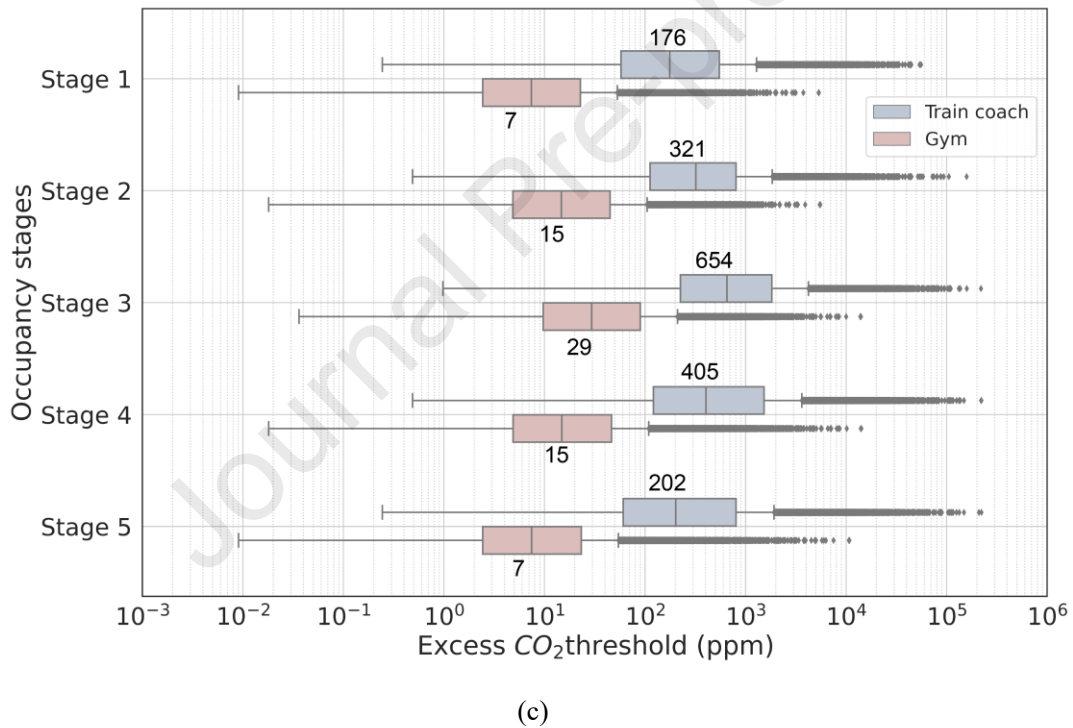
291 Apart from the substantially different C_t among different cases, large uncertainty of C_t was
292 also found in each case, spanning up to six orders of magnitude on a log scale (see Figure 1).
293 Figure 1 shows that cases with a large median value contain more uncertainty due to a more
294 right-shifted log-scaled distribution of C_t , indicating that C_t can be more affected by the
295 uncertainty of emission settings considered in our study. Considering the large uncertainty of
296 C_t and the non-normal distribution when transformed to a linear scale, the median safe excess
297 CO_2 threshold (C_{t50}) is an appropriate descriptive statistic for excess CO_2 threshold due to its

298 high probability density (see the violin plot in Figure 1) (Jones et al., 2021).

299



300



301

302

303 **Figure 1.** Safe excess CO₂ thresholds for 3 scenarios: (a) Scenario 1 (with fixed occupancy);

304 (b) Scenario 2 (with changing occupancy but fixed infection ratios); (c) Scenario 3 (with

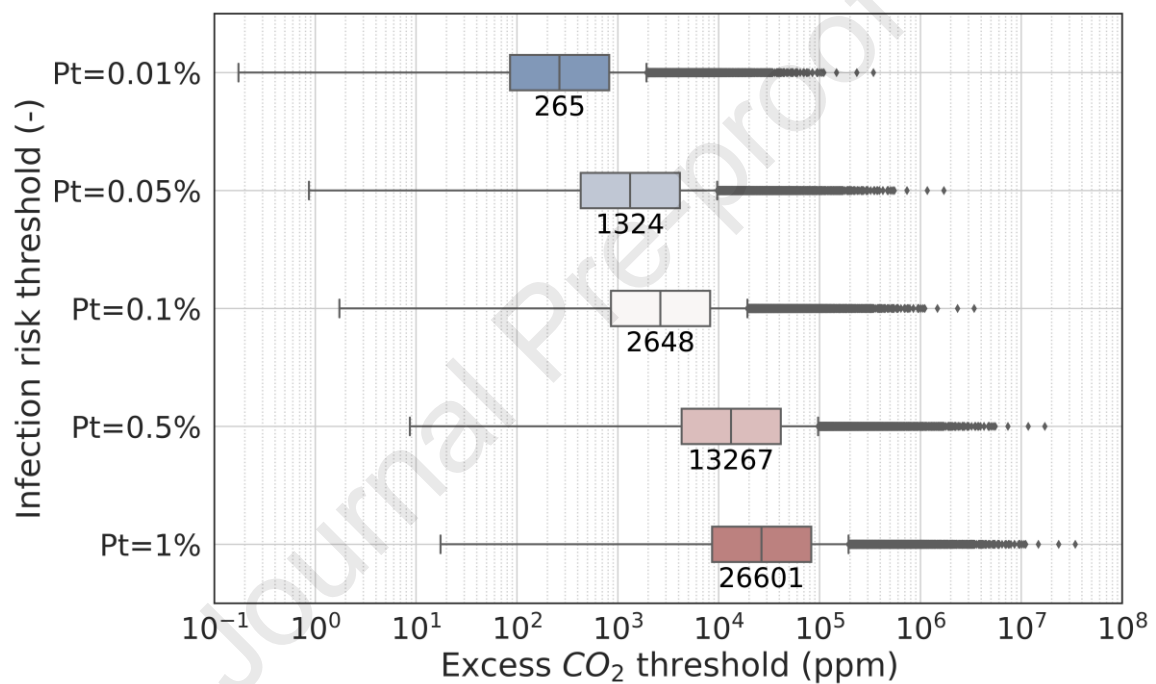
305 changing occupancy and non-fixed infection ratios).

306 3.2 Effect of infection risk threshold (P_t)

307 As discussed before, the infection risk threshold (P_t) plays a role in deriving C_t . Different P_t

308 have been adopted in different research in the range of 0.01% to 1% (Buonanno et al., 2020b;
 309 Dai and Zhao, 2020; Peng and Jimenez, 2021; Zhang et al., 2021). Here we explore how P_t will
 310 affect C_t with results shown in Figure 2. The base case is the classroom in Scenario 1 (see Table
 311 2). C_{t50} is found to be approximately linearly related to P_t with approx. 270 ppm for $P_t = 0.01\%$
 312 to 27000 ppm for $P_t = 1\%$, which reveals the high sensitivity of C_{t50} to P_t .

313



314 **Figure 2.** Excess CO_2 thresholds for the classroom (see Table 2) under different infection risk
 315 thresholds.

316 3.3 Effect of Initial Conditions

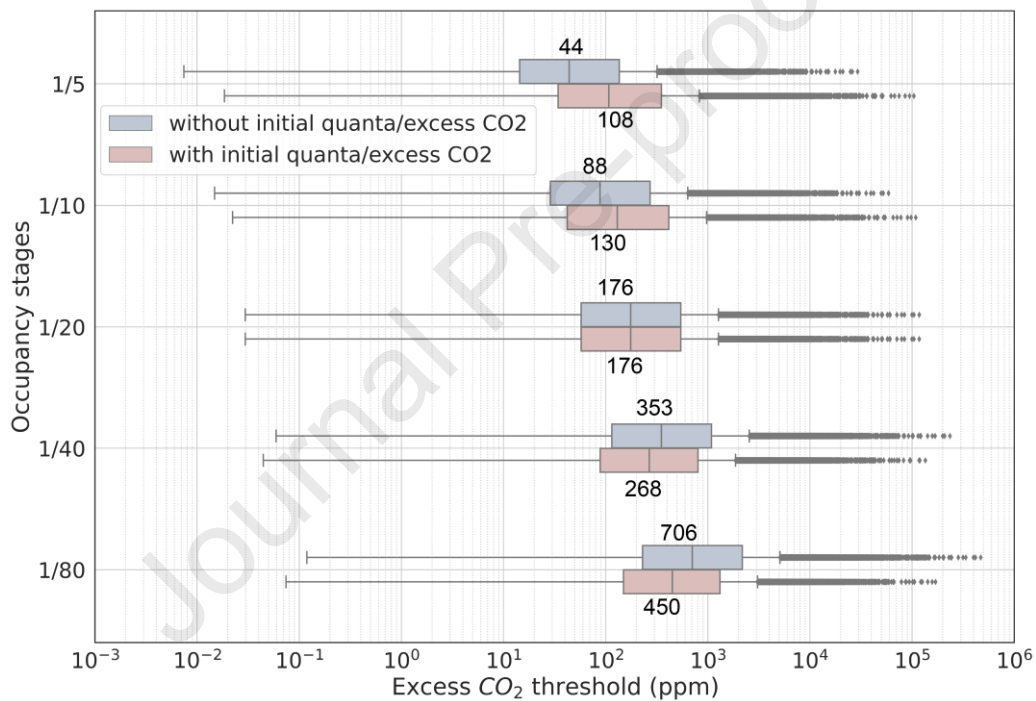
317 We have shown that initial condition of quanta and excess CO_2 can affect the derived safe
 318 excess CO_2 threshold when infection ratio varies among the occupancy stages. However, most
 319 previous studies overlook the initial condition of quanta and excess CO_2 in C_t derivation (Hou
 320 et al., 2021; Peng and Jimenez, 2021; Rudnick and Milton, 2003). To further quantify the

321 impact of initial condition of quanta/excess CO_2 on C_t when infection ratio varies, we compare
322 two cases: 1) considering the initial condition of quanta/excess CO_2 ; 2) no initial quanta/excess
323 CO_2 . We consider two cases with the same indoor volume of 300 m^3 , being occupied both with
324 two stages. The occupants in the two cases are assumed to have “sedentary activity – breathing”,
325 and only 1 infector is adopted.

326 Case 1 assumes there are 20 occupants in Stage 1, and the occupant number in Stage 2
327 changes to 5, 10, 20, 40, 80 respectively, which means the infection ratio will change from $1/20$
328 (Stage 1) to $1/5$, $1/10$, $1/20$, $1/40$, $1/80$ (Stage 2) accordingly and initial quanta/excess CO_2 can
329 affect C_t in Stage 2 in varying degrees. Case 2 assumes there are no occupants in Stage 1 (hence
330 no initial quanta/excess CO_2), and 5 different occupancy levels are assumed for Stage 2 just
331 like case 1. Here we aim to derive C_t for Stage 2 for both two cases with consideration of the
332 impacts of initial quanta/excess CO_2 from Stage 1 (case 1) and without (case 2). The differences
333 of results between the two cases can be used to quantify the impact of initial quanta/excess CO_2
334 on C_t . It's easy to derive C_t for case 2 as there are no initial quanta/excess CO_2 , while for case
335 1, an estimation of initial quanta/excess CO_2 released from stage 1 is needed. Considering the
336 excess CO_2 concentration is affected by different factors such as exposure time and ACH during
337 Stage 1, here we assumed a constant value for initial excess CO_2 concentration for Stage 2 in
338 case 1, namely, 1000 ppm. Initial quanta can then be derived based on it and infection ratios of
339 Stage 1 (see Eq. S4 in Supplementary).

340 Figure 3 shows there are distinct differences of derived C_t between the cases with and
341 without considering initial quanta/excess CO_2 when infection ratio of Stage 2 differs from
342 Stage 1 ($1/20$), suggesting the initial condition of quanta/excess CO_2 shouldn't be ignored in

343 C_t derivation. Overall, when infection ratio increases (larger than 1/20) from Stage 1, C_t
 344 considering initial condition is larger than that without considering initial quanta/excess CO_2 ,
 345 and vice versa. The difference will be higher when the infection ratio deviates more from the
 346 base case of 1/20. When the infection ratio increases from 1/20 (Stage 1) to 1/5 (Stage 2), C_{t50}
 347 increases by 60 ppm than that without considering initial quanta/excess CO_2 and when the
 348 Stage 2 infection ratio decreases from 1/20 to 1/80, C_{t50} becomes 260 ppm lower.
 349



350 **Figure 3.** Excess CO_2 threshold of the second occupancy stage of an indoor space (300 m^3)
 351 under different infection ratios considering with and without initial quanta/ CO_2

352 4. Discussion

353 4.1. New understanding of rebreathed-fraction model

354 RF-based Wells-Riley model proposed by Rudnick and Milton's (2003) used CO_2 as a marker

355 for exhaled-breath exposure and avoided ACH estimation for airborne infection risk
356 assessment. The model does not require any knowledge about ACH, hence it has been widely
357 used in assessing airborne infection risk (Andrews et al., 2014; Hella et al., 2017; Richardson
358 et al., 2014; Wood et al., 2014; Zürcher et al., 2020). However, However, we proved that RF-
359 based model should be only adopted for spaces with fixed occupancy otherwise initial quanta
360 will cause bias of it (see Part 3.3), but this is largely overlooked by many other studies. For
361 spaces with varying occupancy, the initial quanta/excess CO_2 generated by previous occupants
362 but remaining in the air can be very important determining the overall quanta/excess CO_2
363 concentration for next-stage occupancy. How will RF-based model deal with initial
364 quanta/excess CO_2 for spaces with changing occupancy has not been adequately discussed
365 before. In this article, we made analytical derivation to explain the mechanism of RF-based
366 method in dealing with initial quanta/excess CO_2 . We showed that initial quanta/excess CO_2
367 can be considered within the RF-based method in C_t derivation for Scenario 1 (with fixed
368 occupancy) and Scenario 2 (with changing occupancy but fixed infection ratios). This further
369 extends the generalization of RF-based model from spaces with fixed occupancy to spaces with
370 changing occupancy. It should be noted that other recent studies (Burridge et al., 2021; Vouriot
371 et al., 2021) resonate with our study in that they apply RF-based model to spaces with varying
372 occupancy levels to assess infection risk. However, only two occupancy modes were
373 considered in these studies, occupied and non-occupied, which are both included in our
374 Scenario 1. In this contribution, we have proved that for spaces with both occupied and non-
375 occupied modes, the non-occupied period does not affect the proportion of quanta
376 concentration to excess CO_2 concentration in future occupied period if infection ratios remain

377 unchanged given only ventilation is considered here (see Supplementary Information).

378 4.2. Implications for C_t determination

379 Great uncertainty in C_t can be caused by the uncertainty of emissions (E_q and E_{CO_2}) (see
380 Figure 1). E_{CO_2} and E_q contain uncertainty because they have interindividual variation and can
381 be affected by factors such as age, gender (Buonanno et al., 2020a; Persily and de Jonge, 2017;
382 Good et al., 2021). The value of E_q can vary by up to 3 orders of magnitude (e.g., 0.32-240
383 quanta/h for speaking under light activity) (Buonanno et al., 2020a) while E_{CO_2} varies within
384 only one order of magnitude (e.g., 2.88-43.2 L/h) (Persily and de Jonge, 2017). Different
385 studies adopted very different values of E_q and therefore could lead to very different C_t . For
386 only the classroom settings with the same activity level, the median value of E_q in our study is
387 0.37 quanta/h (Buonanno et al., 2020a), while it was in the range of 27.55 quanta/h to 100
388 quanta/h in other studies (Bazant et al., 2021; Hou et al., 2021; Peng and Jimenez, 2021),
389 resulting in several hundred times lower C_t than our results.

390 The choice of P_t and I_t have also an impact C_t . Theoretically, lower P_t can promise safer
391 indoor environment, but this would come at the cost of very low C_t practically impossible to
392 achieve in real-world scenarios. E.g., a low level of C_t may require a very high ACH, unfeasible
393 and prone to cause large energy cost due to the diminishing return phenomenon of ventilation
394 (Li et al., 2021). Besides, how to determine the infector number I_t is also important as it is
395 related to the total quanta emission. Our study defined I_t to be the maximum value of $\{1, P_t N_i\}$
396 as the worst-case scenario. On the contrary, Bazant et al. (2021) considered I_t to be the
397 minimum value of $\{1, P_t N_i\}$, which resulted in a dramatically large C_t (even larger than 10000

398 ppm) when P_I is small.

399 4.3. Implications for infection risk monitoring and control

400 Our model has practical significance for indoor transmission monitoring and control. For
401 Scenario 1 and Scenario 2, safe excess CO_2 threshold is related to variables such as occupancy
402 level, duration and risk threshold through simple equations (see Equation (9) and Equation
403 (12)), making it possible to apply our model for infection risk monitoring in Scenario 1 and 2
404 for public individuals. For instance, when arriving at a space such as a shopping center (as our
405 Scenario 2), people can easily measure the indoor excess CO_2 level first through a portable
406 low-cost CO_2 sensor, then by replacing C_I in Equation (12) by the measured data, people can
407 roughly obtain a safe exposure duration for that shopping center based on their acceptable risk
408 threshold to guide how long they should stay in the shopping center. Furthermore, taking into
409 account the impact of initial quanta/excess CO_2 on risk estimation and C_I derivation, our model
410 can be adopted to further develop different ventilation control strategies such as CO_2 -based
411 demand-controlled ventilation (Li and Cai, 2022) or intermittent ventilation strategy (Melikov
412 et al., 2020; Zhang et al., 2022) with an objective to reduce indoor transmission risk by treating
413 indoor excess CO_2 as a control variable.

414 Further applying our calculation framework into real-world scenarios, some insights can be
415 gained by comparing derived C_I with measurement data/standard limits. For Scenario 1, the
416 occupant numbers can largely affect C_I level, thus, it's warranted to concurrently consider CO_2
417 level and occupant level in transmission risk evaluation of an indoor environment. For example,
418 for classrooms in Scenario 1, the measured excess CO_2 level was found to be in the range of

419 300 - 2500 ppm (outdoor level of 420 ppm) dependent on the number of occupants (Bakó-Biró
420 et al., 2012; Vouriot et al., 2021; Persily et al., 2022). According to our framework, 300 ppm
421 can represent an unsafe environment if the occupant number is less than 33, and 2500 ppm can
422 still be a safe level if occupants is larger than 278. Therefore, C_t threshold should be used in
423 conjunction with occupant number. For scenario 2, community prevalence can dominate C_t and
424 can be used as a reference for lockdown policy implementation. It was found that the one-hour
425 average CO_2 level of 40% shopping mall in Hong Kong exceeded 1000 ppm (Li et al., 2001).
426 To keep infection risk no more than 0.01% for shopping malls, a community prevalence of less
427 than 0.09% is needed according to our calculation framework, otherwise, such places should
428 be locked down. For Scenario 3, taking a restaurant ($\sim 350 \text{ m}^3$) for example, considering two
429 occupancy stage ($N_1 = 20$ for Stage 1 and $N_2 = 80$ for Stage 2) (Shen et al., 2021), according to
430 ASHRAE 62.1 (ASHRAE, 2019), the maximum excess CO_2 limits (the steady-state excess
431 CO_2 concentration under the required ventilation rate) for the first two occupancy stages are
432 540 ppm (Stage 1) and 790 ppm (Stage 2) respectively. But C_t calculated from our framework
433 amounts to 180 ppm and 610 ppm, respectively. The difference indicates the target of infection
434 risk control should be integrated into present ventilation standards to promise both a high level
435 of IAQ and a low infection risk.

436 4.4. Limitation of the study

437 Our study is based on the assumption that outdoor ventilation is the only loss mechanism
438 for quanta in Scenario 1 and Scenario 2, which results in a constant proportion between quanta
439 concentration and excess CO_2 concentration, hence making RF-based model suitable for

440 deriving C_t for Scenario 1 and 2. However, surface deposition, filtration and virus deactivation
441 could significantly contribute to reduce quanta concentration (Blocken et al., 2021; Su et al.,
442 2021; van Doremalen et al., 2020). Neglecting these loss mechanisms may overestimate indoor
443 quanta concentration and result in a lower estimate of C_t than needed. However, the reliability
444 of the derived C_t for a safe indoor environment would not be affected.

445 The thresholds we derived are based on the assumption of a well-mixed room air. Thus, the
446 location of CO_2 sensors needs to be carefully selected to adequately reflect indoor CO_2
447 conditions (Mahyuddin and Awbi, 2010; Mahyuddin et al., 2014). Additionally, our results only
448 account for long-range airborne transmission neglecting the contribution of short-range
449 transmission (Chen et al., 2021; Gao et al., 2021; Li, 2021). Limiting to monitoring infection
450 risk based on C_t values may not be sufficient. Other intervention measures such as wearing
451 masks and social distancing should be jointly considered to control indoor airborne
452 transmission (Jarvis, 2020; Mittal et al., 2020a; Wagner et al., 2021).

453 Another limitation lies in the application of community prevalence (P_I) in our study. For
454 scenario 1 and scenario 3, P_I is used to determine the indoor infector number, which would
455 cause bias because 1) P_I might be smaller than the real value due to the asymptomatic
456 characteristic of SARS-CoV-2 (Lee et al., 2020; Pollock and Lancaster, 2020); and 2) positive
457 individuals may not be present at public spaces due to mandatory quarantine policy which
458 would lead to a lower indoor infection ratio than P_I . For scenario 2, simply using P_I to represent
459 the indoor infection ratio can lead to underestimate the real indoor infection ratio when the
460 number of occupants is small. Conducting field measurement to estimate the average

461 occupancy level (N_{ave}) and selecting the maximum value of $\{1, N_{ave}P_I\}$ could be an alternative
462 method for defining a convincing infection ratio for scenario 2. In addition, considering P_I is
463 changing during different time periods of pandemic, the indoor infection ratio would need to
464 be updated accordingly.

465 In addition, the uncertainty of C_t estimated by our study may be limited as we only
466 considered the uncertainty in emission settings (i.e., quanta emission rate, CO_2 emission rate)
467 in C_t derivation. Community prevalence P_I may contain uncertainty due to the reasons
468 mentioned above. The uncertainty of it may increase the uncertainty of C_t for Scenario 2 where
469 P_I is a dominating input in C_t derivation, but it may not obviously affect C_t for Scenario 1 and
470 3 because P_I is adopted in C_t derivation only when $P_I N_i > 1$ but the occupancy level (N_i) of
471 most cases in Scenario 1 and 3 is usually low and hence $P_I N_i < 1$. Similar as emission settings,
472 breathing rate can also contain uncertainty due to interindividual differences and factors such
473 as age and gender. In addition, quanta emission rate, CO_2 emission rate and breathing rate may
474 all be correlated to each other (Good et al., 2021). In our study, we simply adopted constant
475 breathing rates for different physical activity levels following the study of Buonanno et al.
476 (2020a) which estimated the quanta emission rate under different physical activity levels.
477 Quanta emission rate and CO_2 emission rate are also inter-related through physical activity
478 level (See Table 1). In future, based on more accurate data, the uncertainty and correlation of
479 those parameters may be further interpreted, and the uncertainty of C_t can be therefore further
480 estimated.

481 **5. Conclusion**

482 A new calculation framework was proposed in this study for deriving safe excess CO_2
483 threshold (C_t) for different spaces with consideration of initial quanta/excess CO_2 and
484 fixed/changing occupancy levels. From our derivation process we found that the proportion of
485 indoor excess CO_2 concentration to quanta concentration is constant for a constant infection
486 ratio (infectors/occupants) of an indoor space. Based on this relationship, RF-based (rebreathed
487 fraction-based) model can be directly applied for infection risk assessment and C_t derivation
488 when infection ratio is constant, but not applicable for the cases with varying infection ratios.

489 Affected by factors such as occupant number (N_i), community prevalence (P_l) and activity
490 level, the median value C_{150} derived by our framework varies significantly among the selected
491 cases, with a minimum value of 7 ppm for gym to a maximum value of 890 ppm for lecture
492 hall, with long-tailed distributions. Initial quanta/excess CO_2 is found to largely affect C_t
493 especially when the infection ratio varies significantly among the occupancy stages. A bias of
494 several hundred ppm (e.g., 260 ppm for a space of 300 m³ and with sedentary activity level)
495 could be made if the initial quanta in C_t derivation is not well considered. Our finding illustrates
496 that different CO_2 thresholds should be derived for different spaces and different occupancy
497 stages, rather than being fixed at a constant value for all spaces.

498 Large uncertainty was also found in derived thresholds for all cases, spanning approximately
499 6 orders of magnitude, which are mainly influenced by quanta emission rate (E_q) and CO_2
500 emission rate (E_{CO_2}). For a better control of indoor infection risk through CO_2 monitoring, more
501 accurate input parameters would be needed.

502 **Acknowledgement**

503 XL acknowledged the financial support from China Scholarship Council (CSC) for pursuing
 504 her PhD at the University of Reading, UK.

505 **References**

- 506 Adams, W.C., 1993. Measurement of Breathing Rate and Volume in Routinely Performed Daily
 507 Activities. Final Report. Human Performance Laboratory, Physical Education Department,
 508 University of California, Davis. Human Performance Laboratory, Physical Education
 509 Department, University of California, Davis. Prepared for the California Air Resources
 510 Board, Contract No. A033-205, April 1993.
- 511 Ainsworth, B.E., Haskell, W.L., Whitt, M.C., Irwin, M.L., Swartz, A.M., Strath, S.J., O'Brien,
 512 W.L., Bassett, J., Schmitz, K.H., Emplainscourt, P.O., Jacobs, J., Leon, A.S., 2000.
 513 Compendium of physical activities: An update of activity codes and MET intensities. *Med
 514 Sci Sports Exerc* 32. <https://doi.org/10.1097/00005768-200009001-00009>
- 515 Andrews, J.R., Morrow, C., Walensky, R.P., Wood, R., 2014. Integrating social contact and
 516 environmental data in evaluating tuberculosis transmission in a South African township.
 517 *Journal of Infectious Diseases* 210, 597–603. <https://doi.org/10.1093/infdis/jiu138>
- 518 ASHRAE, 2019. ANSI/ASHRAE Standard 62.1-2019, Ventilation for acceptable indoor
 519 airquality. Peachtree Corners, GA: ASHRAE.
- 520 Bakó-Biró, Z., Clements-Croome, D.J., Kochhar, N., Awbi, H.B., Williams, M.J., 2012.
 521 Ventilation rates in schools and pupils' performance. *Build Environ* 48, 215–223.
 522 <https://doi.org/10.1016/j.buildenv.2011.08.018>
- 523 Bazant, M.Z., Kodio, O., Cohen, A.E., Khan, K., Gu, Z., Bush, J.W.M., 2021. Monitoring
 524 carbon dioxide to quantify the risk of indoor airborne transmission of COVID-19. *Flow* 1,
 525 1–17. <https://doi.org/10.1017/flo.2021.10>
- 526 Blocken, B., van Druenen, T., Ricci, A., Kang, L., van Hooff, T., Qin, P., Xia, L., Ruiz, C.A.,
 527 Arts, J.H., Diepens, J.F.L., Maas, G.A., Gillmeier, S.G., Vos, S.B., Brombacher, A.C.,
 528 2021. Ventilation and air cleaning to limit aerosol particle concentrations in a gym during
 529 the COVID-19 pandemic. *Building and Environment* 193, 107659.
 530 <https://doi.org/10.1016/j.buildenv.2021.107659>
- 531 Buonanno, G., Morawska, L., Stabile, L., 2020a. Quantitative assessment of the risk of airborne
 532 transmission of SARS-CoV-2 infection: Prospective and retrospective applications.
 533 *Environ Int* 145, 106112. <https://doi.org/10.1016/j.envint.2020.106112>
- 534 Buonanno, G., Stabile, L., Morawska, L., 2020b. Estimation of airborne viral emission : Quanta
 535 emission rate of SARS-CoV-2 for infection risk assessment. *Environ Int* 141, 105794.
 536 <https://doi.org/10.1016/j.envint.2020.105794>
- 537 Burrige, H.C., Fan, S., Jones, R.L., Noakes, C.J., Linden, P.F., 2021. Predictive and
 538 retrospective modelling of airborne infection risk using monitored carbon dioxide. *Indoor
 539 and Built Environment* 1420326X2110435. <https://doi.org/10.1177/1420326x211043564>
- 540 CDC, 2021. Ventilation in buildings. Atlanta: Centers for Disease Control and Prevention.
 541 <https://www.cdc.gov/coronavirus/2019-ncov/community/ventilation.html>
- 542 Chen, N., Zhou, M., Dong, X., Qu, J., Gong, F., Han, Y., Qiu, Y., Wang, J., Liu, Y., Wei, Y., Xia,
 543 J., Yu, T., Zhang, X., Zhang, L., 2020. Epidemiological and clinical characteristics of 99

- 544 cases of 2019 novel coronavirus pneumonia in Wuhan, China: a descriptive study. *The*
545 *Lancet* 395, 507–513. [https://doi.org/10.1016/S0140-6736\(20\)30211-7](https://doi.org/10.1016/S0140-6736(20)30211-7)
- 546 Chen, W., Qian, H., Zhang, N., Liu, F., Liu, L., Li, Y., 2022. Extended short-range airborne
547 transmission of respiratory infections. *J Hazard Mater* 422.
548 <https://doi.org/10.1016/j.jhazmat.2021.126837>
- 549 CIBSE, C., 2020. COVID-19 Ventilation Guidance. [https://www.cibse.org/Coronavirus-](https://www.cibse.org/Coronavirus-COVID-19)
550 [COVID-19](https://www.cibse.org/Coronavirus-COVID-19)
- 551 Dai, H., Zhao, B., 2020. Association of the infection probability of COVID-19 with ventilation
552 rates in confined spaces. *Build Simul* 13, 1321–1327. [https://doi.org/10.1007/s12273-](https://doi.org/10.1007/s12273-020-0703-5)
553 [020-0703-5](https://doi.org/10.1007/s12273-020-0703-5)
- 554 EMG/SPI-B, 2021. Application of CO2 monitoring as an approach to managing ventilation to
555 mitigate SARS-CoV-2 transmission. [https://www.gov.uk/government/publications/emg-](https://www.gov.uk/government/publications/emg-and-spi-b-application-of-co2-monitoring-as-an-approach-to-managing-ventilation-to-mitigate-sars-cov-2-transmission-27-may-2021)
556 [and-spi-b-application-of-co2-monitoring-as-an-approach-to-managing-ventilation-to-](https://www.gov.uk/government/publications/emg-and-spi-b-application-of-co2-monitoring-as-an-approach-to-managing-ventilation-to-mitigate-sars-cov-2-transmission-27-may-2021)
557 [mitigate-sars-cov-2-transmission-27-may-2021](https://www.gov.uk/government/publications/emg-and-spi-b-application-of-co2-monitoring-as-an-approach-to-managing-ventilation-to-mitigate-sars-cov-2-transmission-27-may-2021)
- 558 Fang, K.-T., Li, R., Sudjianto, A., 2005. Design and Modeling for Computer Experiments (1st
559 ed.). Chapman and Hall/CRC. <https://doi.org/10.1201/9781420034899>
- 560 Furuya, H., Nagamine, M., Watanabe, T., 2009. Use of a mathematical model to estimate
561 tuberculosis transmission risk in an Internet café. *Environ Health Prev Med* 14, 96–102.
562 <https://doi.org/10.1007/s12199-008-0062-9>
- 563 Gao, C.X., Li, Y., Wei, J., Cotton, S., Hamilton, M., Wang, L., Cowling, B.J., 2021. Multi-route
564 respiratory infection: When a transmission route may dominate. *Science of the Total*
565 *Environment* 752, 141856. <https://doi.org/10.1016/j.scitotenv.2020.141856>
- 566 Gammaitoni, L., Nucci, M. C., 1997. Using a mathematical model to evaluate the efficacy of
567 TB control measures. *Emerging infectious diseases*, 3(3), 335–342.
568 <https://doi.org/10.3201/eid0303.970310>
- 569 Good, N., Fedak, K.M., Goble, D., Keisling, A., L'Orange, C., Morton, E., Phillips, R., Tanner,
570 K., Volckens, J., 2021. Respiratory Aerosol Emissions from Vocalization: Age and Sex
571 Differences Are Explained by Volume and Exhaled CO2. *Environ Sci Technol Lett* 8,
572 1071–1076. <https://doi.org/10.1021/acs.estlett.1c00760>
- 573 Hella, J., Morrow, C., Mhimbira, F., Ginsberg, S., Chitnis, N., Gagneux, S., Mutayoba, B.,
574 Wood, R., Fenner, L., 2017. Tuberculosis transmission in public locations in Tanzania: A
575 novel approach to studying airborne disease transmission. *Journal of Infection* 75, 191–
576 197. <https://doi.org/10.1016/j.jinf.2017.06.009>
- 577 Hou, D., Katal, A., Wang, L. (Leon), Katal, A., Wang, L. (Leon), 2021. Bayesian Calibration
578 of Using CO2 Sensors to Assess Ventilation Conditions and Associated COVID-19
579 Airborne Aerosol Transmission Risk in Schools. *medRxiv* 2021.01.29.21250791.
- 580 Jarvis, M.C., 2020. Aerosol Transmission of SARS-CoV-2: Physical Principles and
581 Implications. *Front Public Health*. <https://doi.org/10.3389/fpubh.2020.590041>
- 582 Jia, W., Wei, J., Cheng, P., Wang, Q., Li, Y., 2022. Exposure and respiratory infection risk via
583 the short-range airborne route. *Build Environ* 219.
584 <https://doi.org/10.1016/j.buildenv.2022.109166>
- 585 Jones, B., Sharpe, P., Iddon, C., Hathway, E.A., Noakes, C.J., Fitzgerald, S., 2021. Modelling
586 uncertainty in the relative risk of exposure to the SARS-CoV-2 virus by airborne aerosol
587 transmission in well mixed indoor air. *Build Environ* 191.

- 588 <https://doi.org/10.1016/j.buildenv.2021.107617>
- 589 Ke, R., Zitzmann, C., Ho, D. D., Ribeiro, R. M., and Perelson, A. S.: In vivo kinetics of SARS-
590 CoV-2 infection and its relationship with a person's infectiousness, *Proc. Natl. Acad. Sci.*
591 U. S. A., 118, <https://doi.org/10.1073/pnas.2111477118>, 2021.
- 592 Ke, R., Martinez, P. P., Smith, R. L., Gibson, L. L., Mirza, A., Conte, M., Gallagher, N., Luo,
593 C. H., Jarrett, J., Zhou, R., Conte, A., Liu, T., Farjo, M., Walden, K. K. O., Rendon, G.,
594 Fields, C. J., Wang, L., Fredrickson, R., Edmonson, D. C., Baughman, M. E., Chiu, K. K.,
595 Choi, H., Scardina, K. R., Bradley, S., Gloss, S. L., Reinhart, C., Yedetore, J., Quicksall,
596 J., Owens, A. N., Broach, J., Barton, B., Lazar, P., Heetderks, W. J., Robinson, M. L.,
597 Mostafa, H. H., Manabe, Y. C., Pekosz, A., McManus, D. D., and Brooke, C. B.: Daily
598 longitudinal sampling of SARS-CoV-2 infection reveals substantial heterogeneity in
599 infectiousness, *Nat Microbiol*, 7, 640-652, 2022.
- 600 Li, B., Cai, W., 2022. A novel CO₂-based demand-controlled ventilation strategy to limit the
601 spread of COVID-19 in the indoor environment. *Build Environ* 219.
602 <https://doi.org/10.1016/j.buildenv.2022.109232>
- 603 Lee, S., Kim, T., Lee, E., Lee, C., Kim, H., Rhee, H., Park, S.Y., Son, H.J., Yu, S., Park, J.W.,
604 Choo, E.J., Park, S., Loeb, M., Kim, T.H., 2020. Clinical Course and Molecular Viral
605 Shedding among Asymptomatic and Symptomatic Patients with SARS-CoV-2 Infection
606 in a Community Treatment Center in the Republic of Korea. *JAMA Intern Med* 180,
607 1447–1452. <https://doi.org/10.1001/jamainternmed.2020.3862>
- 608 Lelieveld, J., Helleis, F., Borrmann, S., Cheng, Y., Drewnick, F., Haug, G., Klimach, T., Sciare,
609 J., Su, H., Pöschl, U., 2020. Model calculations of aerosol transmission and infection risk
610 of covid-19 in indoor environments. *Int J Environ Res Public Health* 17, 1–18.
611 <https://doi.org/10.3390/ijerph17218114>
- 612 Li, W.M., Lee, S.C., Chan, L.Y., 2001. Indoor air quality at nine shopping malls in Hong Kong.
613 *Science of The Total Environment* 273, 27–40. [https://doi.org/10.1016/S0048-](https://doi.org/10.1016/S0048-9697(00)00833-0)
614 [9697\(00\)00833-0](https://doi.org/10.1016/S0048-9697(00)00833-0)
- 615 Li, Y., 2021. Basic routes of transmission of respiratory pathogens—A new proposal for
616 transmission categorization based on respiratory spray, inhalation, and touch. *Indoor Air*.
617 <https://doi.org/10.1111/ina.12786>
- 618 Li, Y., Cheng, P., Jia, W., 2021. Poor ventilation worsens short-range airborne transmission of
619 respiratory infection. *Indoor Air*. <https://doi.org/10.1111/ina.12946>
- 620 Ma, Y., Horsburgh, C.R., White, L.F., Jenkins, H.E., 2018. Quantifying TB transmission: A
621 systematic review of reproduction number and serial interval estimates for tuberculosis.
622 *Epidemiol Infect* 146, 1478–1494. <https://doi.org/10.1017/S0950268818001760>
- 623 Mahyuddin, N., Awbi, H., 2010. The spatial distribution of carbon dioxide in an environmental
624 test chamber. *Build Environ* 45, 1993–2001.
625 <https://doi.org/10.1016/j.buildenv.2010.02.001>
- 626 Mahyuddin, N., Awbi, H.B., Alshitawi, M., 2014. The spatial distribution of carbon dioxide in
627 rooms with particular application to classrooms. *Indoor and Built Environment* 23, 433–
628 448. <https://doi.org/10.1177/1420326X13512142>
- 629 Melikov, A.K., Ai, Z.T., Markov, D.G., 2020. Intermittent occupancy combined with
630 ventilation: An efficient strategy for the reduction of airborne transmission indoors.

- 631 Science of the Total Environment 744. <https://doi.org/10.1016/j.scitotenv.2020.140908>
- 632 Mihi, Mirela, Ani, I.-D., Mihi, M, Professor, F., Ani, I., Kursan Milaković, I., Professor, A.,
633 2018. Time spent shopping and consumer clothing purchasing behaviour EKONOMSKI
634 PREGLED.
- 635 Miller, S.L., Nazaroff, W.W., Jimenez, J.L., Boerstra, A., Buonanno, G., Dancer, S.J., Kurnitski,
636 J., Marr, L.C., Morawska, L., Noakes, C., 2021. Transmission of SARS-CoV-2 by
637 inhalation of respiratory aerosol in the Skagit Valley Chorale superspreading event. *Indoor*
638 *Air* 31, 314–323. <https://doi.org/10.1111/ina.12751>
- 639 Mittal, R., Meneveau, C., Wu, W., 2020a. A mathematical framework for estimating risk of
640 airborne transmission of COVID-19 with application to face mask use and social
641 distancing. *Physics of Fluids* 32. <https://doi.org/10.1063/5.0025476>
- 642 Mittal, R., Ni, R., Seo, J.H., 2020b. The flow physics of COVID-19. *J Fluid Mech* 894.
643 <https://doi.org/10.1017/jfm.2020.330>
- 644 Molina, C., Jones, B., 2021. Investigating Uncertainty in the Relationship between Indoor
645 Steady-State CO₂ Concentrations and Ventilation Rates. *Airc.*
646 <https://doi.org/10.13140/RG.2.2.16867.99361>
- 647 Peng, Z., Jimenez, J.L., 2021. Exhaled CO₂ as a COVID-19 infection risk proxy for different
648 indoor environments and activities. *Environ Sci Technol Lett* 8, 392–397.
649 <https://doi.org/10.1021/acs.estlett.1c00183>
- 650 Peng, Z., Rojas, A. L. P., Kropff, E., Bahnfleth, W., Buonanno, G., Dancer, S. J., Kurnitski, J.,
651 Li, Y., Loomans, M. G. L. C., Marr, L. C., Morawska, L., Nazaroff, W., Noakes, C., Querol,
652 X., Sekhar, C., Tellier, R., Greenhalgh, T., Bourouiba, L., Boerstra, A., Tang, J. W., Miller,
653 S. L., and Jimenez, J. L.: Practical Indicators for Risk of Airborne Transmission in Shared
654 Indoor Environments and Their Application to COVID-19 Outbreaks, *Environ. Sci.*
655 *Technol.*, 56, 1125-1137, 2022.
- 656 Persily, A., de Jonge, L., 2017. Carbon dioxide generation rates for building occupants. *Indoor*
657 *Air* 27, 868–879. <https://doi.org/10.1111/ina.12383>
- 658 Persily, A., Bahnfleth, W., Kipen, H., Lau, J., Mandin, C., Sekhar, C., Wagoocki, P. and Nguyen
659 Weekes, L., 2022, ASHRAE's New Position Document on Indoor Carbon
660 Dioxide, ASHRAE, Journal,
661 https://tsapps.nist.gov/publication/get_pdf.cfm?pub_id=934476
- 662 Riley, E. C., Murphy, G., Riley, R. L., 1978. Airborne spread of measles in a suburban
663 elementary school. *American journal of epidemiology*, 107(5), 421–432.
664 <https://doi.org/10.1093/oxfordjournals.aje.a112560>
- 665 Pollock, A.M., Lancaster, J., 2020. Asymptomatic transmission of covid-19. *The BMJ*.
666 <https://doi.org/10.1136/bmj.m4851>
- 667 Pouwels, K.B., et al., 2021. Community prevalence of SARS-CoV-2 in England from April to
668 November, 2020: results from the ONS Coronavirus Infection Survey. *The Lancet Public*
669 *Health* 6, e30–e38. [https://doi.org/10.1016/S2468-2667\(20\)30282-6](https://doi.org/10.1016/S2468-2667(20)30282-6)
- 670 Qian, H., Miao, T., Liu, L., Zheng, X., Luo, D., Li, Y., 2021. Indoor transmission of SARS-
671 CoV-2. *Indoor Air* 31, 639–645. <https://doi.org/10.1111/ina.12766>
- 672 Rudnick, S.N., Milton, D.K., 2003. Risk of indoor airborne infection transmission estimated
673 from carbon dioxide concentration. *Indoor Air* 13, 237–245.
674 <https://doi.org/10.1034/j.1600-0668.2003.00189.x>

- 675 REHVA, 2021. REHVA COVID-19 Guidance, version 4.1. Brussels, Belgium: Federation of
 676 European Heating, Ventilation and Air Conditioning Associations.
 677 [https://www.rehva.eu/fileadmin/user_upload/REHVA_COVID-](https://www.rehva.eu/fileadmin/user_upload/REHVA_COVID-19_guidance_document_V4.1_15042021.pdf)
 678 [19_guidance_document_V4.1_15042021.pdf](https://www.rehva.eu/fileadmin/user_upload/REHVA_COVID-19_guidance_document_V4.1_15042021.pdf)
- 679 Richardson, E.T., Morrow, C.D., Kalil, D.B., Bekker, L.G., Wood, R., 2014. Shared air: A
 680 renewed focus on ventilation for the prevention of tuberculosis transmission. *PLoS One*
 681 *9*, 1–7. <https://doi.org/10.1371/journal.pone.0096334>
- 682 SAGE-EMG, 2020. EMG: Role of ventilation in controlling SARS-CoV-2 transmission.
 683 [https://www.gov.uk/government/publications/emg-role-of-ventilation-in-controllingsars-](https://www.gov.uk/government/publications/emg-role-of-ventilation-in-controllingsars-cov-2-transmission-30-september-2020)
 684 [cov-2-transmission-30-september-2020](https://www.gov.uk/government/publications/emg-role-of-ventilation-in-controllingsars-cov-2-transmission-30-september-2020)
- 685 Shen, J., Kong, M., Dong, B., Birnkrant, M.J., Zhang, J., 2021. A systematic approach to
 686 estimating the effectiveness of multi-scale IAQ strategies for reducing the risk of airborne
 687 infection of SARS-CoV-2. *Build Environ* *200*.
 688 <https://doi.org/10.1016/j.buildenv.2021.107926>
- 689 Sobol', I.M., 1994. *A Primer for the Monte Carlo Method* (1st ed.). CRC Press.
 690 <https://doi.org/10.1201/9781315136448>
- 691 Su, A., Grist, S.M., Geldert, A., Gopal, A., Herr, A.E., 2021. Quantitative UV-C dose validation
 692 with photochromic indicators for informed N95 emergency decontamination. *PLoS ONE*
 693 *16*, 1–24. <https://doi.org/10.1371/journal.pone.0243554>
- 694 van Doremalen, N., Bushmaker, T., Morris, D.H., Holbrook, M.G., Gamble, A., Williamson,
 695 B.N., Tamin, A., Harcourt, J.L., Thornburg, N.J., Gerber, S.I., Lloyd-Smith, J.O., de Wit,
 696 E., Munster, V.J., 2020. Aerosol and Surface Stability of SARS-CoV-2 as Compared with
 697 SARS-CoV-1. *New England Journal of Medicine* *382*, 1564–1567.
 698 <https://doi.org/10.1056/nejmc2004973>
- 699 Vouriot, C.V.M., Burridge, H.C., Noakes, C.J., Linden, P.F., 2021. Seasonal variation in
 700 airborne infection risk in schools due to changes in ventilation inferred from monitored
 701 carbon dioxide. *Indoor Air* *31*, 1154–1163. <https://doi.org/10.1111/ina.12818>
- 702 Wagner, J., Sparks, T.L., Miller, S., Chen, W., Macher, J.M., Waldman, J.M., 2021. Modeling
 703 the impacts of physical distancing and other exposure determinants on aerosol
 704 transmission. *J Occup Environ Hyg* *1–15*.
 705 <https://doi.org/10.1080/15459624.2021.1963445>
- 706 Wei, J., Li, Y., 2016. Airborne spread of infectious agents in the indoor environment. *Am J*
 707 *Infect Control* *44*, S102–S108. <https://doi.org/10.1016/j.ajic.2016.06.003>
- 708 Wood, R., Morrow, C., Ginsberg, S., Piccoli, E., Kalil, D., Sassi, A., Walensky, R.P., Andrews,
 709 J.R., 2014. Quantification of shared air: A Social and environmental determinant of
 710 airborne disease transmission. *PLoS One* *9*, 1–8.
 711 <https://doi.org/10.1371/journal.pone.0106622>
- 712 Zhang, S., Ai, Z., Lin, Z., 2021. Occupancy-aided ventilation for both airborne infection risk
 713 control and work productivity. *Build Environ* *188*.
 714 <https://doi.org/10.1016/j.buildenv.2020.107506>
- 715 Zhang, S., Niu, D., Lin, Z., 2022. Occupancy-aided ventilation for airborne infection risk
 716 control: Continuously or intermittently reduced occupancies? *Build Simul*.
 717 <https://doi.org/10.1007/s12273-022-0951-7>
- 718 Zürcher, K., Morrow, C., Riou, J., Ballif, M., Koch, A.S., Bertschinger, S., Liu, X., Sharma,

719 M., Middelkoop, K., Warner, D., Wood, R., Egger, M., Fenner, L., 2020. Novel approach
 720 to estimate tuberculosis transmission in primary care clinics in sub-Saharan Africa:
 721 Protocol of a prospective study. *BMJ Open* 10. [https://doi.org/10.1136/bmjopen-2019-](https://doi.org/10.1136/bmjopen-2019-036214)
 722 036214
 723

724 Supplementary Information

725 Derivation Process for Scenario 1 and Scenario 2

726 Scenario 1 and Scenario 2 have constant infection ratios among different occupancy stages, specifically,
 727 $I_1/N_1 = I_2/N_2 = \dots = I_i/N_i$.

728 For S_1 (the start occupancy stage) with no initial quanta and initial excess CO_2 , the solved quanta
 729 concentration ($C_{q,1}$) and excess CO_2 concentration ($C_{CO2,1}$) over time T_1 through mass balance equations can
 730 be expressed as:

$$731 \quad C_{q,1}(t) = -\frac{I_1 E_q}{\lambda_1 V} e^{-\lambda_1 t} + \frac{I_1 E_q}{\lambda_1 V} \quad (S1)$$

$$732 \quad C_{CO2,1}(t) = -\frac{N_1 E_{CO2}}{\lambda_1 V} e^{-\lambda_1 t} + \frac{N_1 E_{CO2}}{\lambda_1 V} \quad (S2)$$

733 A fixed proportion between quanta and excess CO_2 during stage S_1 can be derived:

$$734 \quad \frac{C_{q,1}(t)}{C_{CO2,1}(t)} = \frac{I_1 E_q}{N_1 E_{CO2}} \quad (S3)$$

735 Because initial quanta concentration ($C_{qin,2}$) and initial excess CO_2 concentration ($C_{cin,2}$) for next
 736 occupancy stage S_2 are exactly the concentrations at the end of S_1 , thus, they also have the fixed proportion
 737 relationship as:

$$738 \quad \frac{C_{qin,2}(t)}{C_{cin,2}(t)} = \frac{I_1 E_q}{N_1 E_{CO2}} \quad (S4)$$

739 For S_2 (second occupancy stage), replacing initial quanta concentration ($C_{qin,2}$) by initial excess CO_2
 740 concentration ($C_{cin,2}$) on basis of the fixed proportion above and a constant infection ratio of $I_1/N_1 = I_2/N_2$,
 741 quanta concentration and excess CO_2 concentration over time (T_2) can be expressed as:

$$742 \quad C_{q,2}(t) = \frac{I_2 E_q}{N_2 E_{CO2}} \left((C_{cin,2} - \frac{N_2 E_{CO2}}{\lambda_2 V}) e^{-\lambda_2 t} + \frac{N_2 E_{CO2}}{\lambda_2 V} \right) \quad (S5)$$

$$743 \quad C_{CO2,2}(t) = \left((C_{cin,2} - \frac{N_2 E_{CO2}}{\lambda_2 V}) e^{-\lambda_2 t} + \frac{N_2 E_{CO2}}{\lambda_2 V} \right) \quad (S6)$$

744 A same proportion between quanta and excess CO_2 concentration can be found during occupancy stage
 745 S_2 :

$$746 \quad \frac{C_{q,2}(t)}{C_{CO2,2}(t)} = \frac{I_2 E_q}{N_2 E_{CO2}} \quad (S7)$$

747 If there exists a stage S_0 following stage S_2 that without occupancy (no occupants indoor during period
 748 T_0), quanta and excess CO_2 remained by stage S_2 also experience a synchronously damping in fixed
 749 proportion as S_2 :

$$750 \quad C_{q,0}(t) = \frac{I_2 E_q}{N_2 E_{CO2}} (C_{cin,0} e^{-\lambda_0 t}) \quad (S8)$$

$$751 \quad C_{CO2,0}(t) = C_{cin,0} e^{-\lambda_0 t} \quad (S9)$$

$$752 \quad \frac{C_{q,0}(t)}{C_{CO2,0}(t)} = \frac{I_2 E_q}{N_2 E_{CO2}} \quad (S10)$$

753 Based on constant infection ratios ($I_1/N_1 = I_2/N_2 = \dots = I_i/N_i$), a general analytical expression for quanta

754 concentration and excess CO_2 concentration for stage S_i can be concluded from the derivation process above:

$$755 \quad C_{q,i}(t) = \frac{I_i}{N_i} \frac{E_q}{E_{CO_2}} \left((C_{cin,i} - \frac{N_i E_{CO_2}}{\lambda_i V}) e^{-\lambda_i t} + \frac{N_i E_{CO_2}}{\lambda_i V} \right) \quad (S11)$$

$$756 \quad C_{CO_2,i}(t) = (C_{cin,i} - \frac{N_i E_{CO_2}}{\lambda_i V}) e^{-\lambda_i t} + \frac{N_i E_{CO_2}}{\lambda_i V} \quad (S12)$$

757 For all occupancy stages in Scenario 1 and Scenario 2, quanta concentration and excess CO_2 concentration
758 possess a fixed proportion dominated by three parameters: (1) constant infection ratio; (2) constant quanta
759 emission rate; (2) constant CO_2 emission rate.

$$760 \quad \frac{C_{q,i}(t)}{C_{CO_2,i}(t)} = \frac{I_i}{N_i} \frac{E_q}{E_{CO_2}} \quad (S13)$$

761 Replacing quanta concentration by excess CO_2 concentration, airborne infection risk for stage i can be
762 quantified through Wells-Riley equation based on the excess CO_2 concentration:

$$763 \quad P = 1 - e^{-B \frac{I_i}{N_i} \frac{E_q}{E_{CO_2}} \int_0^{T_i} C_{CO_2,i}(t) dt} \quad (S14)$$

764 Equation (S14) can be converted directly into the classical rebreathed fraction-based infection risk model
765 (Rudnick and Milton, 2003) with $BC_{CO_2}(t)/E_{CO_2}$ representing the rebreathed fraction. Safe excess CO_2
766 threshold for occupancy stage S_i for Scenario 1 and Scenario 2 ($I_i/N_i = P_i$) can then be derived on basis of
767 Equation (S14) with a predefined risk threshold P_i :

$$768 \quad C_t = \frac{E_{CO_2} N_i}{E_q T_i B I_i} \ln \left(\frac{1}{1 - P_t} \right) \quad (S15)$$

769 For each occupancy stage, the initial quanta released by previous stages has been considered in the
770 derivation of safe excess CO_2 threshold in Equation (S15). The application of the derived CO_2 threshold can
771 be extended to more general occupancy stages without limitation of no initial quanta in space.

772

773 Reference

774 Rudnick, S.N., Milton, D.K., 2003. Risk of indoor airborne infection transmission estimated from carbon
775 dioxide concentration. *Indoor Air* 13, 237–245. <https://doi.org/10.1034/j.1600-0668.2003.00189.x>

776

777

778

779

780

781

782

783

Highlights

- Rebreathed fraction-based model can be applied for spaces with changing occupants but constant infection ratios.
- Initial quanta and excess CO_2 lead to bias of determining excess CO_2 threshold when infection ratio changes.
- Excess CO_2 threshold contains large uncertainty and should be determined on a case-by-case basis.

Declaration of interests

The authors declare that they have no known competing financial interests or personal relationships that could have appeared to influence the work reported in this paper.

The authors declare the following financial interests/personal relationships which may be considered as potential competing interests:

Xiaowei Lyu reports financial support was provided by China Scholarship Council.

Journal Pre-proof